

<https://helda.helsinki.fi>

Composition of natural phytoplankton community has minor effects on autochthonous dissolved organic matter characteristics

Haraguchi, Lumi

2019-07-03

Haraguchi , L , Asmala , E , Jakobsen , H H & Carstensen , J 2019 , ' Composition of natural phytoplankton community has minor effects on autochthonous dissolved organic matter characteristics ' , Marine Biology Research , vol. 15 , no. 4-6 , pp. 357-375 . <https://doi.org/10.1080/17451000.2019.1662449>

<http://hdl.handle.net/10138/319174>

<https://doi.org/10.1080/17451000.2019.1662449>

CC BY

acceptedVersion

Downloaded from Helda, University of Helsinki institutional repository.

This is an electronic reprint of the original article.

This reprint may differ from the original in pagination and typographic detail.

Please cite the original version.

**Composition of natural phytoplankton community has minor effects
on autochthonous dissolved organic matter characteristics**

Lumi Haraguchi^{a, b*}; E. Asmala^{c, a}; H. H. Jakobsen^a; and J. Carstensen^a

^a *Department of Bioscience, Aarhus University, Roskilde, Denmark*

^b *Current address: Marine Research Centre, Finnish Environment Institute (SYKE),
Helsinki, Finland*

^c *Tvärminne Zoological Station, University of Helsinki, Hanko, Finland*

Lumi Haraguchi*: lumi.haraguchi@ymparisto.fi

Eero Asmala: eero.asmala@helsinki.fi

Hans H. Jakobsen: hhja@bios.au.dk

Jacob Carstensen: jac@bios.au.dk

* Corresponding author

Acknowledgements

This study was supported by the BONUS COCOA project (Grant Agreement 2112932-1), funded jointly by the EU and Danish Research Council. L.H. was supported by a grant from the Brazilian program Science without Borders/CAPES (Grant No. 13581-13-9). The authors would like to thank Colin Stedmon (DTU Aqua, Denmark) for help with the DOC analysis.

Abstract

Dissolved organic matter (DOM) is an important component of nutrient cycling, but the role of different organisms controlling the processing of autochthonous DOM remains poorly understood. Aiming to characterize phytoplankton-derived DOM and the effects of complex pelagic communities on its dynamics, we incubated natural plankton communities from a temperate mesohaline estuary under controlled conditions for 18 days. The incubations were carried out in contrasting seasons (spring and autumn) and changes in the planktonic community (phytoplankton, bacteria and microzooplankton), nutrients and DOM were assessed. Our results highlight the complexity of DOM production and fate in natural planktonic communities. Small changes in DOM composition were observed in the experiments relative to the orders-of-magnitude variations experienced in the phytoplankton assembly. We argue that the tight coupling between microbial processing and DOM production by phytoplankton and grazers stabilizes variations in quantity and characteristics of autochthonous DOM, resulting in apparently homogeneous semi-labile DOM pool throughout the experiments. However, seasonal differences in the production and processing of DOM were observed, reflecting differences in the nutrient regimes and initial DOM characteristics in each experiment, but also likely influenced by changes in the successional status of the pelagic community. Acknowledging that characteristics of the DOM derived from phytoplankton growth can vary broadly, heterotrophic processing and successional status of the community are synergistically important factors for shaping those characteristics, and thus affecting the seasonal signature of the semi-labile autochthonous DOM pool.

Key words: Pelagic food web; succession; autochthonous DOM

Introduction

Dissolved organic matter (DOM) is an important component of carbon, nitrogen and phosphorus cycling in aquatic systems, operating as storage (Hedges 2002; Jiao et al. 2010) and fuelling heterotrophic organisms through the microbial loop (Azam et al. 1983; Ferrier-Pages & Rassoulzadegan 1994; Cotner & Biddanda 2002). Primary producers have been proposed as an important DOM source in marine ecosystems, notably in those with limited freshwater influence and inputs of allochthonous DOM (Suksomjit et al. 2009), influencing the DOM composition of surface waters (Biddanda & Benner 1997). Phytoplankton can produce DOM (Thornton 2014), with quantity and characteristics varying with nutrient availability (Myklestad 1995), phytoplankton species composition (Biddanda & Benner 1997), and bacterial interaction (Ramanan et al. 2016). From studies with axenic phytoplankton cultures, different taxonomic groups have been found to release different types of DOM (Romera-Castillo et al. 2010; Fukuzaki et al. 2014). Additionally, other biological drivers need to be considered to understand environmental DOM dynamics. For example, grazers can also produce DOM (Strom et al. 1997; Ferrier-Pagès et al. 1998), whereas bacteria consume and alter DOM properties (Rochelle-Newall & Fisher 2002; Romera-Castillo et al. 2011; Kinsey et al. 2018). This complex array of biological processes add up to abiotic ones (e.g. photo degradation), resulting in a DOM pool that becomes less and less reactive (Hansell 2013). Thus, labile DOM is fast transformed into recalcitrant DOM, which encompasses different fractions, whose turnover rates becomes increasingly slower: the semi-labile, semi-refractory, refractory and ultra-refractory fractions (Hansell 2013). As a portion of the DOM absorbs light at UV and visible wavelengths (chromophoric DOM – CDOM), and a fraction of CDOM is fluorescent (FDOM), assessment of the optical properties of the CDOM enables a relatively easy and inexpensive way to

characterize DOM in the environment (Coble 2007; Fellman et al. 2010). Even if the DOM optical properties lack information on the specific molecular structure, the optical properties constitute a proxy for the composition, sources and DOM processing degree (Stubbins et al. 2014). In coastal zones, where the terrestrial influence overlaps intrinsic processes, characterization of DOM sources and cycling can be even more challenging due to high environmental heterogeneity of the pelagic coastal food web (Yamashita et al. 2008). On top of that, DOM exhibits seasonal dynamics, which is partly linked to biological activity (Markager et al. 2011; Knudsen-Leerbeck et al. 2017). Thus, there is a need to advance from describing autochthonous DOM variability to actually understand the underlying processes and mediators (Markager et al. 2011).

This is the second part of a study aimed at characterizing transformations in quantity and characteristics of phytoplankton-derived DOM. Asmala, Haraguchi, Jakobsen, et al. (2018) demonstrated that DOM originating from phytoplankton is rapidly processed and its optical properties are continuously transformed, with dynamics differing strongly over seasons. Phytoplankton composition appeared to have a minor role as driver for the observed DOM dynamics regarding season and inorganic nutrient availability, as the same taxonomical groups (cryptophytes and diatoms) dominated in both seasons (Asmala, Haraguchi, Jakobsen, et al. 2018). Additionally, variations in the DOM quantity were much smaller and were not directly related to variability in phytoplankton biomass (Asmala, Haraguchi, Jakobsen, et al. 2018). The results from Asmala, Haraguchi, Jakobsen, et al. (2018) led us to hypothesize that even if phytoplankton is the primary DOM source, ecological processes, such grazing and succession, are more relevant for the signatures of the semi-labile pool than bulk phytoplankton dynamics.

In this study, we examined the role of plankton community characteristics beyond major phytoplankton groups in order to reveal potential community-driven mechanisms in

DOM transformation, in contrast to the more numerous studies exploring DOM dynamics in phytoplankton monocultures. Our main objective is to evaluate how temporal changes in plankton community structure influence the DOM transformations observed by Asmala, Haraguchi, Jakobsen, et al. (2018). Specifically, we want to evaluate potential effects of changes in community structure in the DOM dynamics at short-term across two different seasons.

Materials & methods

Experiment setup

Roskilde Fjord (RF) is a temperate mesohaline estuary with low freshwater input, albeit rich in nutrients, and it is previously reported to have strong signatures of autochthonous DOM (Knudsen-Leerbeck et al. 2017). The experimental setup was described in detail in Asmala, Haraguchi, Jakobsen, et al. (2018). In summary, surface water (about 80 L) was sampled in the inner basin of RF, screened with a 100 μm mesh to remove large zooplankton, and then transferred within one hour from sampling to six glass jars, each containing 10 L. In three of these experimental units, nitrate (NaNO_3) was added daily (days 0-3), totaling $12 \mu\text{mol L}^{-1}$ nitrate addition. No additions were made to the remaining three control units. The bottles were incubated for 18 days at 10°C and with controlled light (16:8 light: dark cycle, at $100\text{--}120 \mu\text{mol m}^{-2} \text{s}^{-1}$) and constantly stirred with a teflon-coated magnetic bar. The experiment was conducted two times representing contrasting seasons in RF: autumn (from 14 September to 2 October 2015) and spring (14 March to 1 April 2016).

Sampling strategy:

We employed an adaptive sampling strategy in order to follow daily changes in the plankton community and capture significant alterations in nutrients and DOM over the

entire incubation. Samples (100 mL) were taken daily for flow cytometry and FlowCam analysis. Unfortunately, phytoplankton analysis with the flow cytometer was terminated after day 9 in the autumn experiment, due to technical problems with the instrument. *In vivo* fluorescence (ex. 470 / em. 685 nm) of the samples was evaluated daily using a Varian Cary Eclipse fluorometer (Agilent). When major changes were detected in the fluorescence, a more comprehensive sampling was conducted: at days 0, 4, 7, 11, and 18 (spring) and days 0, 4, 8, 14, and 18 (autumn). Comprehensive sampling involved phytoplankton counts by inverted microscopy, chlorophyll *a* extraction (Chla), bacteria abundances, dissolved organic carbon (DOC), chromophoric dissolved organic matter (CDOM), and nutrient concentrations.

Laboratory analyses

Chlorophyll a:

Chla was determined according to the method described by Strickland and Parsons (Strickland & Parsons 1972), following the extraction protocol of Holm-Hansen and Riemann (1978). The extracts were kept at -20°C until measured with an AU 10 Turner field fluorometer (Turner Designs, US). Extracted Chla values were used to validate estimated values from *in vivo* fluorescence.

Flow cytometry:

We employed a pulse-shape recording CytoSense flow cytometer (CytoBuoy.com) to analyse phytoplankton. This technique provides phytoplankton counts (cell sizes 1-1000 µm) comparable to those obtained with traditional microscopy, although with more reliable counts for cells < 5 µm (Haraguchi et al. 2017). Additionally, it also provides

information on cell size and morphology due to its capacity to store the optical profile for each particle, recorded as they travel through the flow cell. The instrument has a 488 nm laser, fluorescence sensors (yellow/green – 550 nm, orange - 600-650 nm, red - 650-700 nm) and two scatter sensors, for light scattered parallel (forward scatter) and orthogonal (sideward scatter) to the incident laser beam. Optical particle profiles from live samples (500 μL – 1000 μL , sampled at a flow rate of 8 $\mu\text{L s}^{-1}$) were collected using the software CytoUSB (CytoBuoy.com), with a threshold of 30 mV for the high sensitivity red fluorescence sensor. This trigger was set to include only particles containing Chla (phytoplankton cells). Recorded cells were clustered according to similarities in their optical properties (length, total Forward Scatter (FWS), total red fluorescence (FLR), total orange fluorescence (FLO), and total Sideward Scatter (SWS)), using the software CytoClus3 (CytoBuoy.com). Particles were assigned to one cluster only and the same clustering algorithm was employed for all samples. Taxonomical information was obtained for some of the clusters based on their optical characteristics, pictures taken by the equipment and cross-referenced with microscopy. Carbon biomass was obtained by converting total FWS to volume (Haraguchi et al. 2017) and then converting volume to biomass using a generic protist volume-to-carbon conversion formula (Menden-Deuer & Lessard 2000). In order to assess phytoplankton physiological state, we estimated the carbon-to-chlorophyll ratio (C:Chla) of each cluster of the phytoplankton community for all samples separately. For this, total carbon biomass was divided by total Chla, which was estimated by converting the total red fluorescence to Chla concentration using an empirical formula proposed by Haraguchi et al. (2017), for the same location where the inoculum were taken. It needs to be emphasised that the carbon and the Chla estimated by CytoSense differs from the carbon and Chla estimated by microscopy and organic solvent extraction method

respectively. Carbon estimates obtained with CytoSense are more precise than microscopy as they are obtained on an individual level (Haraguchi et al. 2017), while CytoSense Chla is based on *in vivo* fluorescence intensity that is more susceptible to physiological changes than Chla (Geider 1987 and references within). Yet, the C:Chla ratio during the experiment is a powerful proxy to follow changes in phytoplankton physiology.

Bacteria:

Bacteria were fixed in glutaraldehyde (1% final concentration) and stored at 4 °C (autumn experiment) and in paraformaldehyde (1% final concentration) and stored at -20 °C (spring) until analysis. For cell counting, bacteria samples were diluted in TE buffer (0.1 M), 10 or 50 times depending on the bacteria concentration. The diluted samples were stained with SYBR green (1:10000 final concentration, Marie et al. 1997) and enumerated by the same equipment employed for the phytoplankton analysis, although with a different set up (200-500 µL, flow rate 8 µL s⁻¹, trigger on 20 mV on the high sensitivity yellow/green 550 nm fluorescence sensor). Heterotrophs were distinguished from phytoplankton by the absence of red fluorescence signal.

FlowCam:

Rotifers and ciliate abundances and body volumes were analysed from live samples using a color FlowCam IV equipped with a FC300 flow cell (Calbet et al. 2014). Samples were kept in dim light at 12 °C and analysed *in vivo* within 4 hours after sampling. The instrument was run in auto image-mode with 4x magnification capturing all particles in the range 15 µm – 1000 µm. The analysis time for each sample was ca. 40 min., corresponding to an analysed volume of 20 mL. After processing the sample, recorded images were manually sorted into ciliates and rotifers. Equivalent Spherical

Diameter (ESD) and body volume were estimated by the software package VISP 3.17 (FluidImagine TM) using the area based diameter (ABD) algorithm of VISP 3.17 (Jakobsen & Carstensen 2011). Carbon biomass was obtained by converting volume to biomass using a generic protist volume-to-carbon conversion formula (Menden-Deuer & Lessard 2000).

Microscopy:

Microscopy counts in this study were only used to support taxonomical identification of the main phytoplankton groups and were linked to the optical signatures of the most important clusters in each experiment. Fixed samples (acidic Lugol's solution, 2-4% final concentration) were analysed from 10-50 mL Utermöhl chambers (Utermöhl 1958), under a size-calibrated inverted microscope (Nikon TI-U, Nikon Instruments Europe B.V.). Sedimented volumes varied depending on the cell concentration. Both phytoplankton and ciliates were enumerated.

Nutrients:

We collected samples for total nutrients, dissolved inorganics, total and total dissolved N and P. Total nutrients (total N; TN and total P; TP) were analysed from unfiltered water samples, whereas dissolved total nutrients (total dissolved N, TDN and total dissolved P, TDP) and inorganic nutrients (nitrite; NO_2^- , nitrate; NO_3^- , ammonium; NH_4^+ , orthophosphate; PO_4^{3-} (DIP) and dissolved inorganic silicate Si) were measured from filtered water samples using combusted GF/F.

Dissolved inorganic nutrient samples were stored frozen in 30 mL acid-washed plastic bottles. The samples were analysed on a San ++ Continuous Flow Analyser (Skalar Analytical B.V, Breda, NL) as previously described (Grasshof 1976; Kaas & Markager

1998). Detection limits were 0.04, 0.1, 0.3, 0.06 and 0.2 $\mu\text{mol L}^{-1}$ for NO_2^- , NO_3^- , NH_4^+ , PO_4^{3-} and Si, respectively.

Samples for total and total dissolved nitrogen (TN and TDN, respectively) and total and total dissolved phosphorus (TP, TDP, respectively) measurements (20 mL) were collected in 30 mL brown glass bottles filled with Milli-Q water prior to sampling. TN and TP were determined by adding oxidants to the sample followed by autoclaving and were analysed on a San ++ Continuous Flow Analyser (Skalar Analytical B.V, Breda, NL). Detection limits for TN and TP were 1.0 $\mu\text{mol N L}^{-1}$ and 0.1 $\mu\text{mol P L}^{-1}$, respectively.

Dissolved inorganic nitrogen (DIN) concentrations were calculated as the sum of the concentrations of NO_2^- , NO_3^- and NH_4^+ . Dissolved organic nutrient concentrations (DON and DOP) were calculated as the difference between total dissolved nutrient (TDN and TDP) and dissolved inorganic nutrient (DIN and DIP).

Dissolved organic carbon (DOC):

DOC was measured with a Shimadzu TOC-VCPH analyser, and the accuracy of measured DOC concentrations was controlled by analysing a seawater reference standard provided by the CRM (consensus reference material) program.

CDOM and FDOM:

CDOM absorption was measured using a Shimadzu 2401PC spectrophotometer with 5 cm quartz cuvette over the spectral range from 200 to 800 nm with 1 nm intervals. Milli-Q (Millipore) water was used as the blank for all samples. Excitation-emission matrices (EEMs) of FDOM were measured with a Varian Cary Eclipse fluorometer (Agilent). A blank sample of ultrapure water was removed from the EEMs, as well as the scattering bands. EEMs were corrected for inner filter effects with absorbance

spectra (Murphy et al. 2010) and Raman calibrated by normalizing to the area under the Raman scatter peak (excitation wavelength of 350 nm) of an ultrapure water sample run on the same session as the samples. The carbon-specific absorbance wavelengths was calculated by dividing the absorbance of a given wavelength λ by the DOC concentration (Weishaar et al. 2003). Here we employed DOC-specific visible absorbance at 440 nm (SVA₄₄₀), which can be used as an estimator of the proportion of visible-absorbing molecules in the DOM pool. FDOM descriptors often used are peaks at specific excitation/emission wavelengths (Coble's peaks), which can be related, for example, to aromatic amino-acids (peak T) or to humic-like substances (peak C) (Coble 1996).

Statistical analyses

Measurements from the experiment were analysed with a linear mixed model that described the effect of treatment over the course of the experiment. Variations in the measurement variable or a log-transform of this (response variable X_{ijk}) were modelled as

$$X_{ijk} = t_i + d_j + t_i \times d_j + e_{ijk} \quad \text{Eq. (1)}$$

where t_i described the overall difference between control and nitrate addition, d_j described the changes for each day, $t_i \times d_j$ described differences over experiment days between the nitrate addition and control, and e_{ijk} described the residual variation among experimental units. The residual error was modelled as an AR(1) process within each experimental unit to account for potential autocorrelation (repeated measures design). The mixed model was analysed separately for the two seasons. Measurements obtained from the flow cytometer and FlowCam showed scale-dependent variations and were log-transformed, whereas measurements of DIN, DIP, Chla and all DOM variables did

not display these tendencies and were assumed approximately normal distributed. Changes in the response variable from one time point to another was calculated as contrasts of parameter estimates of $t_i \times d_j$. The mixed model was analysed using PROC MIXED in SAS version 9.3.

A principal component analysis (PCA) was carried out in order to simplify the multidimensional information on community, facilitating dynamics visualization and interpretation. Community data were log transformed prior to PCA analysis.

Results

Initial conditions

Initial inorganic nutrient concentrations for both spring and autumn experiments were above thresholds considered to limit phytoplankton growth (2.0 μM for DIN and 0.2 μM for DIP), with a N:P ratio around 50 in spring and around 1 in autumn (Fig. 1). DIN was mainly composed of $\text{NO}_2^- + \text{NO}_3^-$ in spring and NH_4^+ in autumn (Fig. 1a, b). Initial Chla levels were substantially higher in spring than autumn (~ 13.5 and $1.8 \mu\text{g L}^{-1}$, respectively; Fig. 2a, b). The phytoplankton community was dominated by cryptophytes (*Teleaulax* spp.) in spring and by a mixed community of cryptophytes (*Teleaulax* spp.) and dinoflagellates (*Heterocapsa* cf. *rotundata* and gymnodinioids) in autumn (Fig. 3). The difference in phytoplankton biomass was paralleled by ciliate biomass of around 40 $\mu\text{g C L}^{-1}$ in spring and 8 $\mu\text{g C L}^{-1}$ in autumn (Fig. 4a, b), with a resulting initial biomass ratio (w/w) between phytoplankton and grazers (ciliates + rotifers) around 60 in spring and 30 in autumn (Fig. 4e, f). Bacterial abundances were similar at the start of the two experiments (Fig. 5), as were the initial planktonic community (Fig. 6). The DOM variables also exhibited distinct characteristics: lower DOC, and peak T, but higher peak C in spring than autumn (Fig. 7 & 8).

Inorganic nutrient dynamics

In spring, DIN and DIP were gradually consumed during the experiment course, although at higher rates at the beginning and end of the experiment (Fig. 1a, c). In autumn, NH_4^+ was the main species of DIN in the control units, and in the treatments, the addition of NO_3^- led to a temporary shift around day 4 in the DIN speciation, although rapidly shifting back to dominance of NH_4^+ during the following days (Fig. 1b). During the autumn experiment beginning, changes in the DIN were significant in the controls (Table 1) due to the consumption on NH_4^+ that was the main inorganic N source (Fig. 1b). Whereas, in the treatments, the NO_3^- additions balanced the NH_4^+ consumption (Fig. 1b), leading to a non-significant change in the resulting DIN during A1 (Table 1). During both seasons, the addition of nitrate stimulated DIP consumption (Fig. 1c, d).

Successional dynamics

Distinct succession phases, manifested by changes in the phytoplankton (composition, biomass and physiological state) and grazer communities, were used to initiate comprehensive sampling during both experiments. These phases were categorized into four types per season, taking into consideration the succession patterns at short-term and seasonal (spring and autumn) scales. The eight phases are described separately and changes in each are summarized in Table 1 and Table SI.

Phase S1 – Expansion (Spring, day 0-4): This phase was characterized by increasing abundance of phytoplankton, dominated by cryptophytes *Teleaulax* spp. (> 80% of the total biomass) and exhibiting a good physiological status, with the lowest C:Chla ratios of the experiment (Fig. 2c). Ciliate biomass also increased fast during this phase (Fig. 4a) with a daily biomass increase of 23 % in the controls and 51% in treatments (Table SI), as did bacterial abundances (Fig. 5a) that almost doubled each day (Table SI). Biomass ratio of phytoplankton to grazers ($\text{r}_{\text{P:G}}$) decreased from 60 to ~15 (Fig. 4e).

Phase S2 – Maturity (Spring, day 5-7): In this phase, phytoplankton biomass peaked and was still dominated by cryptophytes (~70% of the total biomass) (Fig. 3a). However, an increase in the C:Chla ratio was observed (Fig. 2c), with a daily increase of 25% in controls and 19% in treatments (Table 1), indicating a slowing down of the expansive growth. Ciliate biomass remained constant (Fig. 4a), resulting in only minor changes in the $r_{P:G}$ ratio (Fig. 4e). Bacterial abundances declined to levels similar to the initial conditions (Fig. 5a).

Phase S3 – Senescence (Spring, day 8-11): Phytoplankton was still dominated by cryptophytes, yet their biomass was declining ~40% per day (Fig. 3a; Table SI) and diatoms (unidentified pennate diatoms and *Skeletonema* sp.) started to increase in treatments (Fig. 3c). No significant changes were observed for C:Chla, which remained at a high level (Fig. 2c). On the other hand, ciliate biomass declined (Fig. 4a, Table SI), and rotifers started to increase in the treatments (Fig. 4a, c); yet, no change in the $r_{P:G}$ ratio was observed (Fig. 4e). Bacterial abundance increased again, more than two-fold (Fig. 5a).

Phase S4 - Community shift (Spring, day 12-18): Shifts in dominance of phytoplankton (cryptophytes to diatoms, Fig. 3a, c) and grazers (ciliates to rotifers, Fig. 4a, c) were observed. Diatoms increased their biomass until day 14, and then they started to decline (Fig. 3c), reflecting a net increase in C:Chla ratio (Fig. 2c). However, an increase in Chla was observed, which most likely was associated with increasing biomass of miscellaneous nanoflagellates, which resulted in an increase in the $r_{P:G}$ ratio (Fig. 4e). During this phase, experimental units started to behave more erratically, with a large variability in organisms concentrations. Bacterial abundances in the water column continued to increase (Fig. 5a).

Phase A1 – Expansion 2 (Autumn, day 0-4 (control) and 0-5 (treatment)):

Phytoplankton biomass increased (Fig. 3b) due to growth of cryptophytes (*Teleaulax* spp.) and dinoflagellates (*Heterocapsa* cf. *rotundata* + gymnodinioids). In the controls, phytoplankton grew until day 4 and then declined, while in the treatments growth continued onto day 5. The C:Chla ratio remained relatively constant, but started to increase in the controls from day 3 (Fig. 2d). Ciliates grew well in all units, reaching maximum biomasses at day 4 (controls) or day 5 (treatments), resulting in a decrease in the $r_{P:G}$ ratio (Figs. 4b, 4f). Changes in bacteria could not be assessed due to lack of initial data (Fig. 5b).

Phase A2 – Rapid community shift (Autumn, day 4-8 (control) and 5-8 (treatment)): In

contrast to spring, the intermediate phases from expansion to community shift were not observed in autumn. Cryptophytes (Fig. 3b) continued the decline from the expansion phase in the controls, as opposed to the increase in diatoms (mainly *Skeletonema* sp. and a small unidentified centric) from day 4 that was observed in both controls and treatments (Fig. 3d). The C:Chla ratio first increased (drastically for control units) and decreased again after day 5, resulting in a net increase of 18% during this phase and reaching similar levels for treatments and controls at day 7 (Fig. 2d, Table 1). Ciliates declined drastically, with one day delay between control and treatment units (Fig. 4b), whereas rotifers increased rapidly (Fig. 4d). The $r_{P:G}$ ratio remained constant below 10 at first, but rose towards the end of the phase when grazers collapsed (Fig. 4f). Bacterial abundances increased during this period (Fig. 5b).

Phase A3 – Destabilization (Autumn, day 9-14): No high-resolution data from

phytoplankton were available after day nine; however, the decline in phytoplankton was confirmed by Chla values and microscopy counts (data not shown). Grazers and bacteria also declined (Fig. 4b, 4d, 5b).

Phase A4– Regeneration (Autumn, day 15-18): Phytoplankton and grazers were nearly absent. Bacteria abundances decreased in controls (-24% per day), but not in treatments (Fig. 5b, Table SI).

The dynamics of the microbial community were also captured by the PCA, with similar succession patterns being observed in both experiments (Fig. 6). An initial cryptophyte-dominated assembly shifted to diatom-domination. A similar shift was observed for the grazers, with ciliates associated with cryptophytes and rotifers occurring with diatoms (Fig. 6). In spring, the treatments were very similar, while in autumn nitrate additions induced a large change in the biomass (Fig. 2a, b, 3), but smaller changes in the community structure (Fig. 6). Except for the later phase in spring (S4), treatments and seasons exhibited similar trajectories over time. However, differences in the processing velocity were evident from the PCA, with larger distance between days in autumn than in spring, especially during the initial phases (Fig. 6). Unfortunately, data after day 9 were not available for the phytoplankton community in autumn, but Chla data indicated that phytoplankton collapsed after day 9.

DOM dynamics

In spring, two distinct periods could be identified for the DOM pool transformation. One was observed at the initial phases (S1 and S2) and marked by the accumulation of DOC and DON (Fig. 7a, c). In phase S1, an increase in protein-like DOM (peak T) was observed at the same time as reduction of humic-like (peak C), followed by accumulation of peak C in phase S2 (Fig. 8c, e). The second period was marked by the accumulation of CDOM (SVA₄₄₀) during phase S3 (treatment units) and S4 (controls) (Fig. 8a). Although DOP was consumed throughout the incubations, differences in the consumption pattern between treatments were observed, with consumption stagnating in phase S2 (controls) or S3 (treatments).

In autumn, initial changes in the DOM pool were marked by the decline in peak T during the initial phase A1 (Fig. 8f). Significant changes were noticed later in the experiment: increase in DOC (during A3) and peak C (during A4), along with decrease in peak T (during A4) and CDOM (SVA₄₄₀) (during both A3 and A4) (Fig. 7b, 8b, d, f).

Discussion

Coastal ecosystems display seasonal variations in CDOM and DOC associated with phytoplankton spring blooms, but the dynamics and magnitude of CDOM and DOC vary between years and are hypothesized to depend on bloom composition and interaction with heterotrophs (Minor et al. 2006; Suksomjit et al. 2009). Thus, production of autochthonous DOM can be important in estuarine and coastal areas, but the processes and drivers behind autochthonous DOM seasonal variability remains to be further studied (Markager et al. 2011). One major obstacle impeding our understanding of these processes has been the lack of studies with high-frequency sampling for assessing the role of different communities in the coastal ecosystems (for example plankton, as shown in this study) together with changes in the DOM pool, particularly over different seasons. The daily sampling frequency in this work highlights the fast dynamics and tight coupling between phytoplankton and grazers. The observed dynamics in the plankton community would not have been properly described with lower sampling frequency, suggesting that at least daily sampling is needed in experiments with complex natural plankton communities. DOM and nutrients were sampled only at five occasions, as these constituents were considered less variable. Nevertheless, we recognise that our sampling scheme was inadequate to trace the dynamics of the labile DOM pool, which can be processed by bacteria over time spans of hours (Fuhrman & Ferguson 1986). Thus, the DOM variables analysed in this study most likely represent the dynamics of the semi-labile pool, but considering that most of

DOM in marine surface environments can be regarded as semi-labile (Carlson 2002), we believe that our results are representative of natural conditions.

The study site Roskilde Fjord (RF) is a shallow and microtidal temperate estuary, with long freshwater residence time, high nutrient inputs and low freshwater discharge (Kamp-Nielsen 1992; Staehr et al. 2017). Because of those characteristics, RF is an ideal environment for investigating the biogeochemical processing of DOM, since disturbances from physical transport are low and nutrients and carbon are primarily processed within the system (Asmala, Haraguchi, Markager, et al. 2018). RF has contrasting characteristics between spring and autumn, changing from net autotrophic, DIN-rich and DIP-poor in spring to net heterotrophic, DIN-poor and DIP-rich in autumn (Staehr et al. 2017). Concentrations and composition of organic C, N and P pools in RF change substantially over the seasonal scale, displaying a gradual decrease in bioavailable DOC from spring to autumn, whereas the proportions of bioavailable DON and DOP are more variable and possibly related to occurrences of higher phytoplankton biomass (Knudsen-Leerbeck et al. 2017). This highlights the importance of phytoplankton in regulating the composition of DOM associated with different forms of organic N and P. In our experiments, the initial DOM pool had contrasting characteristics between seasons: spring DOM had more allochthonous characteristics and autumn DOM was more autochthonous, most likely related to the higher freshwater inputs during early spring and further processing of DOM over summer (Asmala, Haraguchi, Jakobsen, et al. 2018). The spring bloom in RF is fuelled by inorganic nutrients, mainly from land, whereas summer and autumn production is mainly sustained by nutrient inputs from sediments and occasional intrusions of deeper waters from the Kattegat (Knudsen-Leerbeck et al. 2017; Staehr et al. 2017).

Phytoplankton derived DOM signature: physiological status or species composition?

Phytoplankton grown under replete light and nutrient conditions with constant temperature maintain a constant optimum Chl *a* quota per cell, whereas changing light, temperature and nutrient limitation can lead to substantial variations in cellular Chl *a* (Geider 1987 and references within). Cellular decreasing Chl *a*, or the change in the specific cell ratio in C:Chl *a*, is therefore a proxy for the physiological status of the phytoplankton community and is reflecting the balance between carbon fixation and other growth processes (Fig 2c, d). Under nutrient deplete conditions, the Chl *a* per cell is reduced in order to lower the accumulation of solar energy within the cell to avoid photochemical damage. Yet the cell does not entirely stop photosynthesis, and the cell needs to store the solar energy as photosynthetic products; either as fatty acids or release them to the water as DOM. The excess DOM is either passively diffused or excreted actively, with the dominant process depending on the physiological status of the organism and species (Thornton 2014). The release of DOM by phytoplankton can be enhanced by excess levels of light (Cherrier et al. 2015) and nutrient limitation, with enhanced release of simple carbohydrates under N or P limitation (Mykkestad 1995; Biddanda & Benner 1997). Nutrient status also influences the bioavailability of released DOM compounds, with DOM originating from phytoplankton grown under nutrient-deplete conditions being less bioavailable for bacteria (Obernosterer & Herndl 1995; Puddu et al. 2003).

It has been demonstrated that different phytoplankton species, growing under axenic conditions, produce DOM with distinct quantity and quality, and that DOM production is correlated to phytoplankton abundance (Romera-Castillo et al. 2010; Fukuzaki et al. 2014). In our experiments, similarity between seasons was observed for phytoplankton, with dominance of cryptophytes (*Teleaulax* spp.) in the initial phase, followed by a transition phase to a final diatom-dominated community after nutrient depletion set in

(P in spring and N in autumn). Interestingly, no difference in the bulk DOM and CDOM was observed between phases dominated by different taxonomical groups in any of our experiments. Furthermore, variability in the DOC concentrations was modest in comparison with biomass changes experienced by phytoplankton, and DOC and phytoplankton biomass dynamics were decoupled. Hence, phytoplankton composition and biomass appear to have a secondary role in structuring the bulk and optical DOM characteristics of the semi-labile pool in a complex community.

In spring, during phase S1, cryptophytes dominated the phytoplankton biomass, while an increase in DON and protein-like FDOM (peak T) was observed. During this phase, cryptophytes notably increased their biomass and exhibited good physiological state, indicated by the low C:Chla ratios. Peak T can be used as a proxy for fresh autochthonous DOM (Coble 2007; Hansen et al. 2016), and the exudation of proteinaceous compounds by healthy phytoplankton associated with peak T signal has been described by Romera-Castillo et al. (2010). Bacterial peak T production was also reported, with the largest fraction occurring within the cells rather than in the extracellular phase (Fox et al. 2017). Considering that our FDOM measurements were derived from gently filtered samples, it is reasonable to assume that most of peak T in the experiments was from the dissolved pool. Production rates of FDOM are reported to be higher for bacteria than phytoplankton (Romera-Castillo et al. 2011); yet, in our experiments the increase in peak T was only observed during S1, in contrast to bacteria increases that were observed in other phases (S3, S4 and A2). Thus, the increase in peak T during the spring expansion (S1) phase is most likely linked to phytoplankton growth, either directly or mediated through bacteria. The high initial peak C values indicated allochthonous/terrestrial DOM, which was more labile and readily consumable within the first four days of the experiment (Asmala, Haraguchi, Jakobsen, et al. 2018), as

evidenced by the sharp decline of this variable. This was followed by an increase in peak C of almost similar magnitude between day 4 and 7 (phase S2), which in our closed experimental units could only be associated with autochthonous production. Peaks with optical signatures similar to terrestrial sources (peak A and C) are found to be produced by marine phytoplankton grown under axenic conditions (Romera-Castillo et al. 2010; Fukuzaki et al. 2014) and, notably, by bacteria growing on phytoplankton exudates (Romera-Castillo et al. 2011; Kinsey et al. 2018). We suggest that this accumulation of humic-like substances was more likely derived from bacterial processing of phytoplankton exudates (peak T). Thus, the balance between peak T production and consumption, and autochthonous peak C accumulation appears to be related to the physiological state of the phytoplankton cells and not only the biomass of net autotrophic communities. In the autumn experiment, even though cryptophytes were growing and accounted for ~50% of the phytoplankton biomass in the first phase, a decrease in peak T was observed. We attribute the opposite behaviour of peak T between seasons to differences in the overall metabolic state of the community, which is net autotrophic in spring and net heterotrophic in autumn (Staehr et al. 2017). Asmala, Haraguchi, Jakobsen, et al. (2018) pointed out that differences in the limitation patterns between seasons (P-limited spring and N-limited autumn) also might influence the bacterial efficiency to degrade DOM, with P-surplus in autumn boosting the bacterial capacity to utilize DOM in comparison to spring. Thus, while in spring DIN:DIP ratios were high and production exceeded consumption, a net accumulation of DON and peak T was observed; in autumn, when DIN:DIP was low and heterotrophy predominant, peak T was readily consumed, even if produced, resulting in a net decrease. Those findings suggest that phytoplankton physiology might be more relevant than species composition for the

specific DOM production, whereas the role of phytoplankton for governing the DOM pool is small when other community components are present. This means that the DOM pool in the environment is regulated in synergy by the entire food web / community structure, and not just by the primary producers.

Role of heterotrophs

Although DOM production might be controlled by phytoplankton, the bacterial community is essential in regulating DOM quantities and characteristics in the environment (Guillemette & del Giorgio 2012). Previous studies have demonstrated that bacterial composition and activity are tightly coupled to primary production and that bacterial communities quickly adapt to efficiently use phytoplankton-derived DOM, resulting in modest changes in the DOM pool (Sarmiento & Gasol 2012; Landa et al. 2016; Hoikkala et al. 2016; Luria et al. 2017). In both experiments the proportion of bioavailable DOC was reported to be low, indicating tight food-web coupling and fast bacterial processing of freshly produced DOM in both seasons (Asmala, Haraguchi, Jakobsen, et al. 2018). Thus, we argue that our results display the net effect of planktonic communities on autochthonous DOM dynamics, despite the fact we lack detailed information on bacterial community composition and activity.

In our experiments, changes in the bacterial abundances followed the Chla dynamic in spring, whereas such correspondence was less evident in autumn, indicating a tighter coupling between bacteria and photosynthesis in spring and the importance of other DOM sources in autumn. The biomass proportion between autotrophs and heterotrophs can be used as a proxy for community structure, varying according to resources availability and relative turnover rates of autotrophs and heterotrophs (Gasol et al. 1997). The proportion of autotrophs to grazers ($r_{P:G}$) (Fig. 4e, f) reflected differences in the initial community structure of each experiment, and here we used it as a proxy for

the biomass between auto- and heterotrophs. Differences in $r_{P:G}$ indicate that spring was more autotrophic with slower turnover rates than autumn, further supported by the fast successional transition in the later (Fig. 6). This was also evidenced by the dynamic of the main inorganic nitrogen species in each experiment, with a large contribution of NH_4^+ to DIN indicating the importance of heterotrophic regeneration processes, especially in autumn.

Although it was not possible to distinguish the effects of grazing from other processes in our experiments, we argue that grazing was essential to fuel the microbial loop, especially during autumn, and likely contributed to the DOM pool dynamic. In addition, the intense ciliate grazing on cryptophytes, probably opened a niche for diatom growth, as ciliates preferentially graze on nanoflagellates rather than large and colonial diatoms (Kivi & Setälä 1995; Granéli & Turner 2002; Sommer et al. 2005). It is not possible to conclude whether the shift observed in phytoplankton community in both experiments was driven by nutrient limitation or grazing, and most likely it was due to a combination of both. Interestingly, diatoms grew after inorganic nutrient depletion (phase S4 and A2), which could be due to association with bacteria, remineralising nutrients in the surrounding phycosphere around the diatom cells (Amin et al. 2012). Although no significant effects of phytoplankton composition was observed in our experiments, the increased contribution of diatoms likely marked the shift from water column processes to processes related to surfaces (i.e. suspended particles, detritus, marine snow). In mature communities the substrates become more important and particle-attached life strategies become dominant, as the external nutrient inputs are limited and recycled nutrients drive the system production (Wetzel 1995). Thus, the faster development of the autumn experiment and the occurrence of the later phases (destabilisation and regeneration, phase A3 and A4, respectively) probably reflect the higher dependency of

the mature communities on nutrient recycling, and therefore on heterotrophic and microbial nutrient processing. Those mature stages were not reached during the spring experiments, due to the slower turnover rates.

Differences in the autotrophs, heterotrophs and $r_{P:G}$ at the beginning and during each experiment were not reflected to the same extent in the DOM pool. This can be attributed to the intricate dynamic between nutrients and the pelagic community, resulting in DOM that is constantly produced, but differing by the dominant origin process (Kujawinski 2011). This can be exemplified for the mesohaline Chesapeake Bay, where similar rates of DON release over different seasons were observed, although DON was mainly released from autotrophs in May switching to be released by heterotrophs in October (Bronk et al. 1998). Similar to this study, our experiments showed that nitrate-rich and -poor conditions likely favoured DOM production directly from phytoplankton and mediated by grazers, respectively. Hence, our results suggest that nutrient conditions are the main controlling factor for the balance between autotrophic and heterotrophic processes of DOM production; however, these processes tend to produce DOM with similar bulk and optical characteristics, giving the impression of DOM resilience. This suggests that the semi-labile DOM pool measured with our methods is relatively resilient to changes in phytoplankton composition, biomass and physiological state. As parts of the DOM pool are very reactive and can change over time scales of hours (Kirchman et al. 1991; Obernosterer et al. 2008), the fast responses of the microbial and phytoplankton communities seem to stabilise DOM optical characteristics. This implies that tightly coupled microbial processing counterbalances large changes in the phytoplankton community and, most likely, the associated production of DOM. On the other hand, the resilient DOM pool might

change slowly over the season resulting in a seasonal signature that reflects the gradually changing composition and status of the community.

Plankton succession and the reactivity of autochthonous DOM

Characteristics of marine DOM are a result from its origin and processing history, comprising a mixed pool of molecules, with different degree of availability to bacteria and other organisms. As labile autochthonous DOM is rapidly consumed, the resulting DOM pool is increasingly recalcitrant as the heterotrophic degradation continues (Benner 2002). Although most of the DOM components in our experiments are considered somehow resistant to biological transformation, the experiments exhibited changes in DOM characteristics with divergent trajectories over the experiments, indicating that DOM was continuously processed (Asmala, Haraguchi, Jakobsen, et al. 2018). In spring, most changes occurred during the first half of the experiment, while in autumn most of the changes were observed at the end of the experiment (Asmala, Haraguchi, Jakobsen, et al. 2018). In this study, we show that those changes in the DOM pool were related to phytoplankton production (spring) and remineralisation (autumn). The role of successional changes in our experiments was further supported by the net increase of DOC concentrations in both experiments, accompanied by contrasting patterns between seasons for CDOM, with net accumulation in spring and consumption in autumn (Asmala, Haraguchi, Jakobsen, et al. 2018). In this study, we highlight the CDOM dynamic by including DOC-specific visible absorbance (SVA₄₄₀), which also showed net increase in spring and decrease in autumn. The SVA₄₄₀ dynamics showed that changes in the CDOM pool were not gradually occurring over the course of the experiments, but at specific successional stages of the community, primarily associated with phytoplankton decay. In spring, a drastic CDOM accumulation was observed in phases S3 (treatment units) and S4 (controls), following

the collapse of the cryptophytes and ciliates populations. In autumn, a CDOM decrease was only observed after the planktonic community collapsed (phases A3 and A4) and when a large amount of DOC was released. This indicates that in autumn, the planktonic community was likely producing DOM that was quickly processed and after the community collapse, bacteria had only more recalcitrant CDOM available, resulting in the accumulation of recalcitrant DOC. This could also explain the magnitude of the observed changes in both experiments, where terrestrial DOM associated with net primary productivity and slower turnover rates in spring would promote larger changes in the DOM pool as it would be more labile. Conversely, the background DOM in autumn is likely to be more recalcitrant, as it has been exposed to degradation over summer, and as the turnover rates of the community are also faster, any fresh DOM produced would be quickly processed. However, when the pelagic community collapsed, the microbial community had to process the more recalcitrant DOM, leading to delayed and smaller changes in the pool in comparison to spring. Those results suggest that over the annual cycle, along with the succession of planktonic communities, the DOM pool follows the reactivity continuum, driven by the patterns in nutrient availability. Our results are aligned with the concept that new nutrients stimulate net community production leading to accumulation of non-labile DOM that has been previously described for Roskilde Fjord (Asmala, Haraguchi, Jakobsen, et al. 2018) and for larger scales (Hansell & Carlson 1998; Romera-Castillo et al. 2016). However, in this study we emphasize the complexity of DOM processing by natural communities, showing that species composition (for both autotrophs and heterotrophs) play a secondary role for determining signatures of environmental DOM, as species composition in nature result from community development and maturity (in response to nutrient limitation), and dilution of water masses. Analysing changes in DOM in light of

the community successional stages might provide a better framework for interpreting autochthonous DOM processing in a broad range of environmental conditions, not only over the seasonal but also at spatial scales.

Conclusions

Phytoplankton composition and biomass appear to have a minor effect on changes in the bulk and optical characteristics of DOM, when heterotrophic community components (grazers and bacteria) are present. We provide a comprehensive view on the summarised complex processing of the autochthonous DOM produced by autotrophs in the environment in contrast to experiments with axenic cultures or monocultures. Our results suggest that the successional stages of diverse biological communities have an effect on DOM cycling in coastal areas and that this community effect should be considered in studies of environmental DOM. Our results indicate that even if phytoplankton photosynthesis is the primary initial source of DOM, the extent of subsequent heterotrophic processing and the ecological status of the community, which are related to patterns in nutrient limitation, ultimately governs the flow of DOM in natural environments and the seasonal signature of the semi-labile and recalcitrant autochthonous DOM pool.

References

- Amin SA, Parker MS, Armbrust E V. 2012. Interactions between Diatoms and Bacteria. *Microbiol Mol Biol Rev* [Internet]. 76:667–684. Available from: <http://mmbr.asm.org/cgi/doi/10.1128/MMBR.00007-12>
- Asmala E, Haraguchi L, Jakobsen HH, Massicotte P, Carstensen J. 2018. Nutrient availability as major driver of phytoplankton-derived dissolved organic matter transformation in coastal environment. *Biogeochemistry*. 137:93–104.

640 Asmala E, Haraguchi L, Markager S, Massicotte P, Riemann B, Staehr PA, Carstensen
 641 J. 2018. Eutrophication Leads to Accumulation of Recalcitrant Autochthonous Organic
 642 Matter in Coastal Environment. *Global Biogeochem Cycles* [Internet]. [cited 2019 Jan
 643 3]; 32:1673–1687. Available from:
 644 <https://onlinelibrary.wiley.com/doi/abs/10.1029/2017GB005848>
 645 Azam F, Fenchel T, Field J, Gray J, Meyer-Reil L, Thingstad F. 1983. The Ecological
 646 Role of Water-Column Microbes in the Sea. *Mar Ecol Prog Ser* [Internet]. 10:257–263.
 647 Available from: <http://www.int-res.com/articles/meps/10/m010p257.pdf>
 648 Benner R. 2002. Chemical Composition and Reactivity. In: Hansell D, Carlson C,
 649 editors. *Biogeochem Mar Dissolved Org Matter* [Internet]. 2nd ed. [place unknown]:
 650 Elsevier; [cited 2017 Nov 13]; p. 59–90. Available from:
 651 <http://linkinghub.elsevier.com/retrieve/pii/B9780123238412500051>
 652 Biddanda B, Benner R. 1997. Carbon, nitrogen, and carbohydrate fluxes during the
 653 production of particulate and dissolved organic matter by marine phytoplankton. *Limnol*
 654 *Oceanogr.* 42:506–518.
 655 Bronk DA, Gilbert PM, Malone TC, Banahan S, Sahlsten E. 1998. Inorganic and
 656 organic nitrogen cycling in Chesapeake Bay: Autotrophic versus heterotrophic
 657 processes and relationships to carbon flux. *Aquat Microb Ecol.* 15:177–189.
 658 Calbet A, Sazhin AF, Nejstgaard JC, Berger SA, Tait ZS, Olmos L, Sousoni D, Isari S,
 659 Martínez RA, Bouquet J-M, et al. 2014. Future Climate Scenarios for a Coastal
 660 Productive Planktonic Food Web Resulting in Microplankton Phenology Changes and
 661 Decreased Trophic Transfer Efficiency. Ianora A, editor. *PLoS One* [Internet]. [cited
 662 2017 Nov 6]; 9:e94388. Available from:
 663 <http://dx.plos.org/10.1371/journal.pone.0094388>

664 Carlson CA. 2002. Production and Removal Processes. In: Hansell DA, Carlson CA,
 665 editors. *Biogeochem Mar Dissolved Org Matter*. 2nd ed. [place unknown]: Elsevier; p.
 666 91–151.

667 Cherrier J, Valentine SK, Hamill B, Jeffrey WH, Marra JF. 2015. Light-mediated
 668 release of dissolved organic carbon by phytoplankton. *J Mar Syst* [Internet]. 147:45–51.
 669 Available from: <http://dx.doi.org/10.1016/j.jmarsys.2014.02.008>

670 Coble PG. 1996. Characterization of marine and terrestrial DOM in seawater using
 671 excitation-emission matrix spectroscopy. *Mar Chem* [Internet]. [cited 2017 Nov 13];
 672 51:325–346. Available from:
 673 <http://www.sciencedirect.com/science/article/pii/0304420395000623>

674 Coble PG. 2007. Marine optical biogeochemistry: The chemistry of ocean color. *Chem*
 675 *Rev*. 107:402–418.

676 Cotner JB, Biddanda BA. 2002. Small players, large role: Microbial influence on
 677 biogeochemical processes in pelagic aquatic ecosystems. *Ecosystems*. 5:105–121.

678 Fellman JB, Hood E, Spencer RGM. 2010. Fluorescence spectroscopy opens new
 679 windows into dissolved organic matter dynamics in freshwater ecosystems: A review.
 680 *Limnol Oceanogr* [Internet]. 55:2452–2462. Available from:
 681 <http://doi.wiley.com/10.4319/lo.2010.55.6.2452>

682 Ferrier-Pagès C, Karner M, Rassoulzadegan F. 1998. Release of dissolved amino acids
 683 by flagellates and ciliates grazing on bacteria. *Oceanol Acta*. 21:485–494.

684 Ferrier-Pages C, Rassoulzadegan F. 1994. N remineralization in planktonic protozoa.
 685 *Limnol Oceanogr* [Internet]. 39:411–419. Available from:
 686 <http://doi.wiley.com/10.4319/lo.1994.39.2.0411>

687 Fox BG, Thorn RMS, Anesio AM, Reynolds DM. 2017. The in situ bacterial production
 688 of fluorescent organic matter; an investigation at a species level. *Water Res* [Internet].
 689 [cited 2019 Jan 3]; 125:350–359. Available from:
 690 <https://linkinghub.elsevier.com/retrieve/pii/S0043135417307029>

691 Fuhrman J, Ferguson R. 1986. Nanomolar concentrations and rapid turnover of
 692 dissolved free amino acids in seawater: agreement between chemical and
 693 microbiological measurements. *Mar Ecol Prog Ser* [Internet]. [cited 2017 Nov 10];
 694 33:237–242. Available from: <http://www.jstor.org/stable/24825448>

695 Fukuzaki K, Imai I, Fukushima K, Ishii KI, Sawayama S, Yoshioka T. 2014.
 696 Fluorescent characteristics of dissolved organic matter produced by bloom-forming
 697 coastal phytoplankton. *J Plankton Res.* 36:685–694.

698 Gasol JM, del Giorgio PA, Duarte CM. 1997. Biomass distribution in marine planktonic
 699 communities. *Limnol Oceanogr* [Internet]. 42:1353–1363. Available from:
 700 <http://dx.doi.org/10.4319/lo.1997.42.6.1353>

701 Geider RJ. 1987. Light and temperature dependence of the carbon to chlorophyll a ratio
 702 in microalgae and cyanobacteria: implications for physiology and growth of
 703 phytoplankton. *New Phytol* [Internet]. [cited 2017 Nov 21]; 106:1–34. Available from:
 704 <http://doi.wiley.com/10.1111/j.1469-8137.1987.tb04788.x>

705 Granéli E, Turner J. 2002. Top-down regulation in ctenophore-copepod-ciliate-diatom-
 706 phytoflagellate communities in coastal waters: a mesocosm study. *Mar Ecol Prog Ser.*
 707 239:57–68.

708 Grasshof K. 1976. *Methods of Seawater Analysis* [Internet]. Grasshoff K, editor.
 709 Weinheim, Germany: Verlag Chemie; [cited 2017 Nov 6]. Available from:
 710 <http://doi.wiley.com/10.1002/9783527613984>

711 Guillemette F, del Giorgio PA. 2012. Simultaneous consumption and production of
 712 fluorescent dissolved organic matter by lake bacterioplankton. *Environ Microbiol*
 713 [Internet]. [cited 2019 Jan 3]; 14:1432–1443. Available from:
 714 <http://doi.wiley.com/10.1111/j.1462-2920.2012.02728.x>

715 Hansell DA. 2013. Recalcitrant Dissolved Organic Carbon Fractions. *Ann Rev Mar Sci*
 716 [Internet]. [cited 2019 Jan 9]; 5:421–445. Available from:
 717 <http://www.annualreviews.org/doi/10.1146/annurev-marine-120710-100757>

718 Hansell DA, Carlson CA. 1998. Net community production of dissolved organic carbon.
 719 *Global Biogeochem Cycles* [Internet]. [cited 2019 Jan 4]; 12:443–453. Available from:
 720 <http://doi.wiley.com/10.1029/98GB01928>

721 Hansen AM, Kraus TEC, Pellerin BA, Fleck JA, Downing BD, Bergamaschi BA. 2016.
 722 Optical properties of dissolved organic matter (DOM): Effects of biological and
 723 photolytic degradation. *Limnol Oceanogr* [Internet]. 61:1015–1032. Available from:
 724 <http://doi.wiley.com/10.1002/lno.10270>

725 Haraguchi L, Jakobsen H, Lundholm N, Carstensen J. 2017. Monitoring natural
 726 phytoplankton communities: a comparison between traditional methods and pulse-shape
 727 recording flow cytometry. *Aquat Microb Ecol* [Internet]. [cited 2017 Oct 18]; 80:77–92.
 728 Available from: <http://www.int-res.com/abstracts/ame/v80/n1/p77-92/>

729 Hedges JI. 2002. Why Dissolved Organic Matter. In: Hansell D, Carlson CA, editors.
 730 *Biogeochem Mar Dissolved Org Matter* [Internet]. [place unknown]: Elsevier; [cited
 731 2017 Oct 18]; p. 1–33. Available from:
 732 <http://linkinghub.elsevier.com/retrieve/pii/B9780123238412500038>

733 Hoikkala L, Tammert H, Lignell R, Eronen-Rasimus E, Spilling K, Kisand V. 2016.
 734 *Autochthonous Dissolved Organic Matter Drives Bacterial Community Composition*

during a Bloom of Filamentous Cyanobacteria. *Front Mar Sci* [Internet]. [cited 2017 Dec 12]; 3:111. Available from: <http://journal.frontiersin.org/Article/10.3389/fmars.2016.00111/abstract>

Holm-Hansen O, Rieman B. 1978. Chlorophyll a Determination: Improvements in Methodology. *Oikos* [Internet]. [cited 2017 Nov 6]; 30:438. Available from: <http://www.jstor.org/stable/3543338?origin=crossref>

Jakobsen HH, Carstensen J. 2011. FlowCAM: Sizing cells and understanding the impact of size distributions on biovolume of -planktonic community structure. *Aquat Microb Ecol.* 65:75–87.

Jiao N, Herndl GJ, Hansell DA, Benner R, Kattner G, Wilhelm SW, Kirchman DL, Weinbauer MG, Luo T, Chen F, Azam F. 2010. Microbial production of recalcitrant dissolved organic matter: long-term carbon storage in the global ocean. *Nat Rev Microbiol* [Internet]. [cited 2017 Oct 18]; 8:593–599. Available from: <http://www.nature.com/doifinder/10.1038/nrmicro2386>

Kaas H, Markager S. 1998. Technical guidelines for marine monitoring. [Internet]. [place unknown]. Available from: <http://bios.au.dk/videnudveksling/til-myndigheder-og-saerligt-interesserede/fagdatacentre/fdcmarintny/tekniske-anvisninger-nova-1998/>

Kamp-Nielsen L. 1992. Benthic-pelagic coupling of nutrient metabolism along an estuarine eutrophication gradient. In: Hart BT, Sly PG, editors. *Sediment/Water Interact* [Internet]. Dordrecht: Springer Netherlands; [cited 2018 Feb 27]; p. 457–470. Available from: http://www.springerlink.com/index/10.1007/978-94-011-2783-7_39

Kinsey JD, Corradino G, Ziervogel K, Schnetzer A, Osburn CL. 2018. Formation of Chromophoric Dissolved Organic Matter by Bacterial Degradation of Phytoplankton-Derived Aggregates. *Front Mar Sci* [Internet]. 4:1–16. Available from:

759 <http://journal.frontiersin.org/article/10.3389/fmars.2017.00430/full>

760 Kirchman DL, Suzuki Y, Garside C, Ducklow HW. 1991. High turnover rates of
 761 dissolved organic carbon during a spring phytoplankton bloom. *Lett to Nat.* 352:612–
 762 614.

763 Kivi K, Setälä O. 1995. Simultaneous measurement of food particle selection and
 764 clearance rates of planktonic oligotrich ciliates (Ciliophora: Oligotrichina). *Mar Ecol*
 765 *Prog Ser.* 119:125–138.

766 Knudsen-Leerbeck H, Mantikci M, Bentzon-Tilia M, Traving SJ, Riemann L, Hansen
 767 JLS, Markager S. 2017. Seasonal dynamics and bioavailability of dissolved organic
 768 matter in two contrasting temperate estuaries. *Biogeochemistry.* 134:217–236.

769 Kujawinski EB. 2011. The Impact of Microbial Metabolism on Marine Dissolved
 770 Organic Matter. *Ann Rev Mar Sci* [Internet]. 3:567–599. Available from:
 771 <http://www.annualreviews.org/doi/10.1146/annurev-marine-120308-081003>

772 Landa M, Blain S, Christaki U, Monchy S, Obernosterer I. 2016. Shifts in bacterial
 773 community composition associated with increased carbon cycling in a mosaic of
 774 phytoplankton blooms. *ISME J.* 10:39–50.

775 Luria CM, Amaral-Zettler LA, Ducklow HW, Repeta DJ, Rhyne AL, Rich JJ. 2017.
 776 Seasonal shifts in bacterial community responses to phytoplankton-derived dissolved
 777 organic matter in the Western Antarctic Peninsula. *Front Microbiol.* 8:1–13.

778 Marie D, Partensky F, Jacquet S, Vault D. 1997. Enumeration and Cell Cycle Analysis
 779 of Natural Populations of Marine Picoplankton by Flow Cytometry Using the Nucleic
 780 Acid Stain SYBR Green I. *Applied environmental Microbiol.* 63:186–193.

781 Markager S, Stedmon CA, Søndergaard M. 2011. Seasonal dynamics and conservative

782 mixing of dissolved organic matter in the temperate eutrophic estuary Horsens Fjord.
 783 Estuar Coast Shelf Sci [Internet]. [cited 2017 Nov 13]; 92:376–388. Available from:
 784 <http://www.sciencedirect.com/science/article/pii/S0272771411000242#fig2>

785 Menden-Deuer S, Lessard EJ. 2000. Carbon to volume relationships for dinoflagellates,
 786 diatoms, and other protist plankton. *Limnol Oceanogr.* 45:569–579.

787 Minor EC, Simjouw J-P, Mulholland MR. 2006. Seasonal variations in dissolved
 788 organic carbon concentrations and characteristics in a shallow coastal bay. *Mar Chem*
 789 [Internet]. 101:166–179. Available from:
 790 <http://linkinghub.elsevier.com/retrieve/pii/S0304420306000405>

791 Murphy KR, Butler KD, Spencer RGM, Stedmon CA, Boehme JR, Aiken GR. 2010.
 792 Measurement of Dissolved Organic Matter Fluorescence in Aquatic Environments: An
 793 Interlaboratory Comparison. *Environ Sci Technol* [Internet]. [cited 2018 Jan 22];
 794 44:9405–9412. Available from: <http://pubs.acs.org/doi/abs/10.1021/es102362t>

795 Myklestad SM. 1995. Release of extracellular products by phytoplankton with special
 796 emphasis on polysaccharides. *Sci Total Environ.* 165:155–164.

797 Obernosterer I, Christaki U, Lefèvre D, Catala P, Van Wambeke F, Lebaron P. 2008.
 798 Rapid bacterial mineralization of organic carbon produced during a phytoplankton
 799 bloom induced by natural iron fertilization in the Southern Ocean. *Deep Res Part II Top*
 800 *Stud Oceanogr.* 55:777–789.

801 Obernosterer I, Herndl GJ. 1995. Phytoplankton extracellular release and bacterial
 802 growth: dependence on the inorganic N:P ratio. *Mar Ecol Prog Ser* [Internet]. [cited
 803 2017 Nov 23]; 116:247–257. Available from: [http://www.int-](http://www.int-res.com/articles/meps/116/m116p247.pdf)
 804 [res.com/articles/meps/116/m116p247.pdf](http://www.int-res.com/articles/meps/116/m116p247.pdf)

805 Puddu A, Zoppini A, Fazi S, Rosati M, Amalfitano S, Magaletti E. 2003. Bacterial
806 uptake of DOM released from P-limited phytoplankton. *FEMS Microbiol Ecol.* 46:257–
807 268.

808 Ramanan R, Kim BH, Cho DH, Oh HM, Kim HS. 2016. Algae-bacteria interactions:
809 Evolution, ecology and emerging applications. *Biotechnol Adv* [Internet]. 34:14–29.
810 Available from: <http://dx.doi.org/10.1016/j.biotechadv.2015.12.003>

811 Rochelle-Newall EJ, Fisher TR. 2002. Production of chromophoric dissolved organic
812 matter fluorescence in marine and estuarine environments: an investigation into the role
813 of phytoplankton. *Mar Chem.* 77:7–21.

814 Romera-Castillo C, Letscher RT, Hansell DA. 2016. New nutrients exert fundamental
815 control on dissolved organic carbon accumulation in the surface Atlantic Ocean. *Proc*
816 *Natl Acad Sci U S A* [Internet]. [cited 2019 Jan 4]; 113:10497–502. Available from:
817 <http://www.ncbi.nlm.nih.gov/pubmed/27582464>

818 Romera-Castillo C, Sarmiento H, Álvarez-Salgado XA, Gasol JM, Marrasé C. 2010.
819 Production of chromophoric dissolved organic matter by marine phytoplankton. *Limnol*
820 *Oceanogr* [Internet]. 55:446–454. Available from:
821 <http://www.scopus.com/inward/record.url?eid=2-s2.0-75749143410&partnerID=40&md5=94935160c398371d667a2beeeeca292d>

823 Romera-Castillo C, Sarmiento H, Alvarez-Salgado XA, Gasol JM, Marrasé C. 2011.
824 Net production and consumption of fluorescent colored dissolved organic matter by
825 natural bacterial assemblages growing on marine phytoplankton exudates. *Appl Environ*
826 *Microbiol.* 77:7490–7498.

827 Sarmiento H, Gasol JM. 2012. Use of phytoplankton-derived dissolved organic carbon
828 by different types of bacterioplankton. *Environ Microbiol.* 14:2348–2360.

829 Sommer U, Hansen T, Blum O, Holzner N, Vadstein O, Stibor H. 2005. Copepod and
830 microzooplankton grazing in mesocosms fertilised with different Si:N ratios: No
831 overlap between food spectra and Si:N influence on zooplankton trophic level.
832 *Oecologia*. 142:274–283.

833 Staehr PA, Testa J, Carstensen J. 2017. Decadal Changes in Water Quality and Net
834 Productivity of a Shallow Danish Estuary Following Significant Nutrient Reductions.
835 *Estuaries and Coasts* [Internet]. 40:63–79. Available from:
836 <http://link.springer.com/10.1007/s12237-016-0117-x>

837 Strickland JDH, Parsons TR. 1972. A practical handbook of seawater analysis. Ottawa:
838 Fisheries Research Board of Canada.

839 Strom SL, Benner R, Ziegler S, Dagg MJ. 1997. Planktonic grazers are a potentially
840 important source of marine dissolved organic carbon. *Limnol Oceanogr*. 42:1364–1374.

841 Stubbins A, Lapierre JF, Berggren M, Prairie YT, Dittmar T, Del Giorgio PA. 2014.
842 What's in an EEM? Molecular signatures associated with dissolved organic
843 fluorescence in boreal Canada. *Environ Sci Technol*. 48:10598–10606.

844 Suksomjit M, Nagao S, Ichimi K, Yamada T, Tada K. 2009. Variation of dissolved
845 organic matter and fluorescence characteristics before, during and after phytoplankton
846 bloom. *J Oceanogr*. 65:835–846.

847 Thornton DCO. 2014. Dissolved organic matter (DOM) release by phytoplankton in the
848 contemporary and future ocean. *Eur J Phycol* [Internet]. [cited 2015 Jan 12]; 49:20–46.
849 Available from: <http://www.tandfonline.com/doi/abs/10.1080/09670262.2013.875596>

850 Utermöhl H. 1958. Zur Vervollkommnung der quantitativen Phytoplankton-Methodik :
851 Mit 1 Tab. Internatio. Stuttgart: Schweizerbart.

852 Weishaar JL, Aiken GR, Bergamaschi BA, Fram MS, Fujii R, Kenneth M. 2003.
 853 Evaluation of Specific Ultraviolet Absorbance as an Indicator of the Chemical
 854 Composition and Reactivity of Dissolved Organic Carbon. *Environ Sci Technol*
 855 [Internet]. [cited 2017 Nov 13]; 37:4702–4708. Available from:
 856 <http://pubs.acs.org/doi/abs/10.1021/es030360x>

857 Wetzel RG. 1995. Death, detritus, and energy flow in aquatic ecosystems. *Freshw Biol*
 858 [Internet]. [cited 2018 Dec 19]; 33:83–89. Available from:
 859 <http://doi.wiley.com/10.1111/j.1365-2427.1995.tb00388.x>

860 Yamashita Y, Jaffé R, Maie N, Tanoue E. 2008. Assessing the dynamics of dissolved
 861 organic matter (DOM) in coastal environments by excitation emission matrix
 862 fluorescence and parallel factor analysis (EEM-PARAFAC). *Limnol Oceanogr.*
 863 53:1900–1908.
 864
 865

Table 1: Significant rates of change ($P < 0.05$) derived from the repeated measures mixed model for the different phases of the two seasonal experiments. Rates were estimated as the difference between start and end day divided by number of days. Non-significant rates ($P > 0.05$) are not shown. Phases with a significant change in rates between control (C) and treatment (T) are shaded in grey.

Spring experiment	Phases							
	S1		S2		S3		S4	
	C	T	C	T	C	T	C	T
DIN ($\mu\text{M d}^{-1}$)	-6.17	-3.11					-3.71	-3.81
DIP ($\mu\text{M d}^{-1}$)	-0.19	-0.20			-0.06	-0.06		
Chla ($\mu\text{g L}^{-1} \text{d}^{-1}$)	2.82	2.16	-2.72	-2.43	-2.74		2.91	2.26
C:Chla (% d^{-1})			25%	19%	-13%		-11%	
DOC ($\mu\text{M d}^{-1}$)								
DON ($\mu\text{M d}^{-1}$)			4.05					
DOP ($\mu\text{M d}^{-1}$)				-0.05	-0.04			
SVA ₄₄₀ ($\text{m}^2 \text{g}^{-1} \text{C d}^{-1}$)	-0.004		0.008			0.035	0.017	-0.003
Autumn experiment	A1		A2		A3		A4	
	C	T	C	T	C	T	C	T
DIN ($\mu\text{M d}^{-1}$)	-0.80			-1.53				0.92
DIP ($\mu\text{M d}^{-1}$)	-0.14	-0.19		-0.33			0.15	0.16
Chla ($\mu\text{g L}^{-1} \text{d}^{-1}$)		1.47		1.25	-0.48	-1.78		
C:Chla (% d^{-1})		23%	18%		-28%			
DOC ($\mu\text{M d}^{-1}$)					22.21	38.91		
DON ($\mu\text{M d}^{-1}$)	2.31		-3.19					
DOP ($\mu\text{M d}^{-1}$)								
SVA ₄₄₀ ($\text{m}^2 \text{g}^{-1} \text{C d}^{-1}$)			-0.005			-0.005	-0.005	-0.004

Figure 1. Dissolved inorganic nutrients concentrations during the course of the experiment in spring (left column) and autumn (right column) experiments. Dashed horizontal lines indicate nutrient thresholds potentially limiting phytoplankton growth ($2.0 \mu\text{mol L}^{-1}$ for DIN and $0.2 \mu\text{mol L}^{-1}$ for DIP). Note the difference in scaling between spring and autumn experiments. Error bars show maximum and minimum of replicated units. The different phases observed in the experiments are indicated with shaded background.

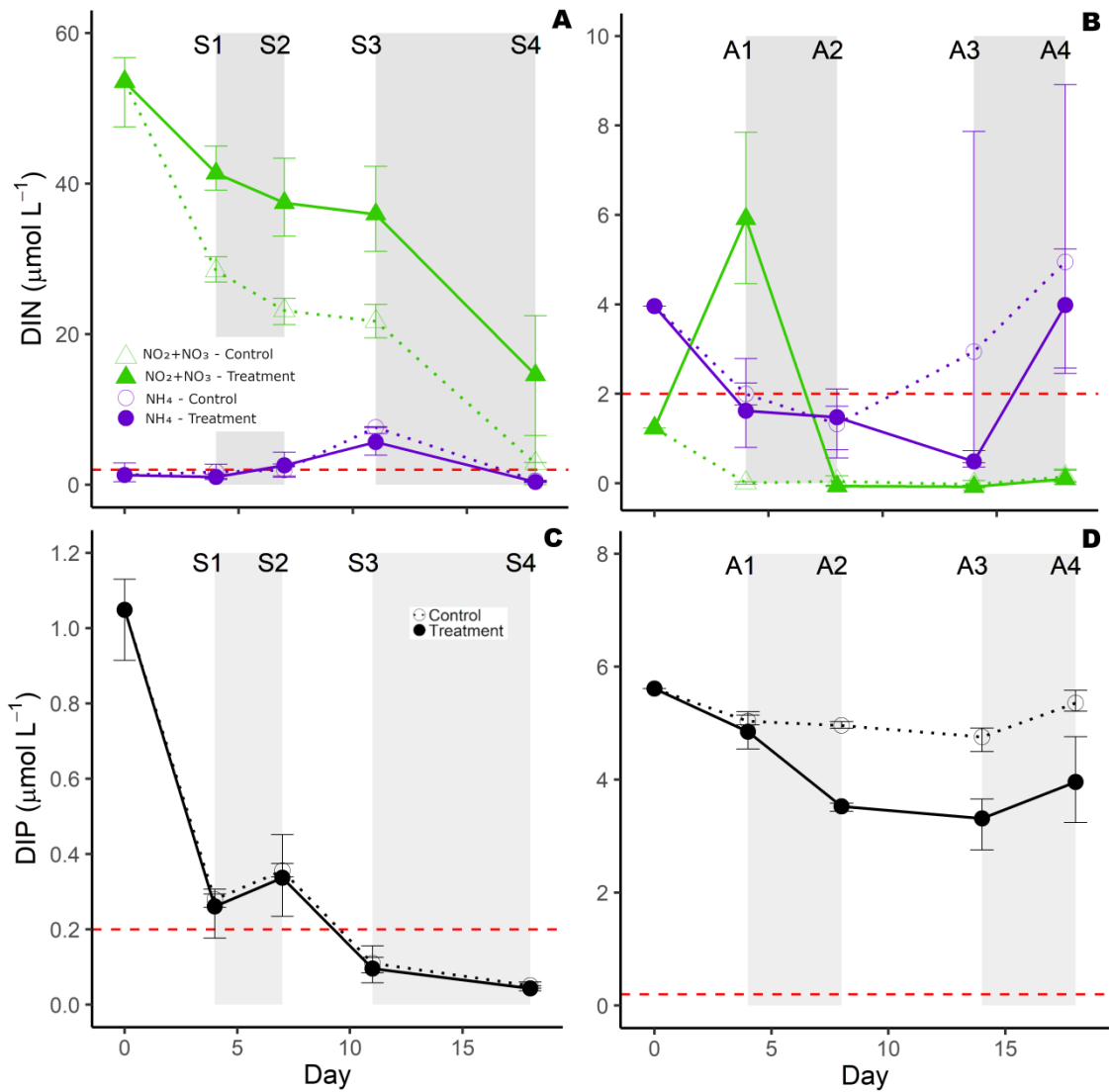
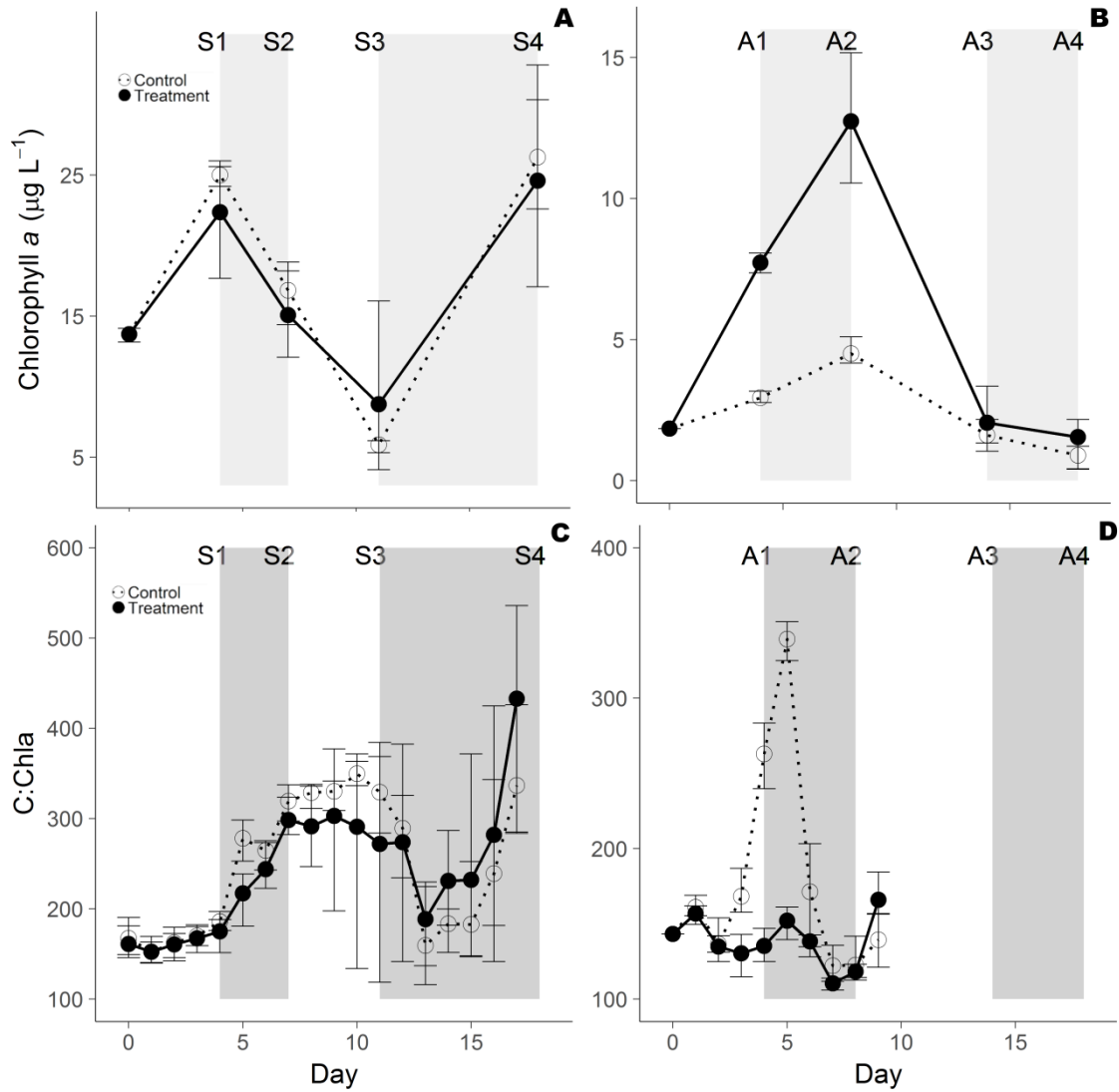
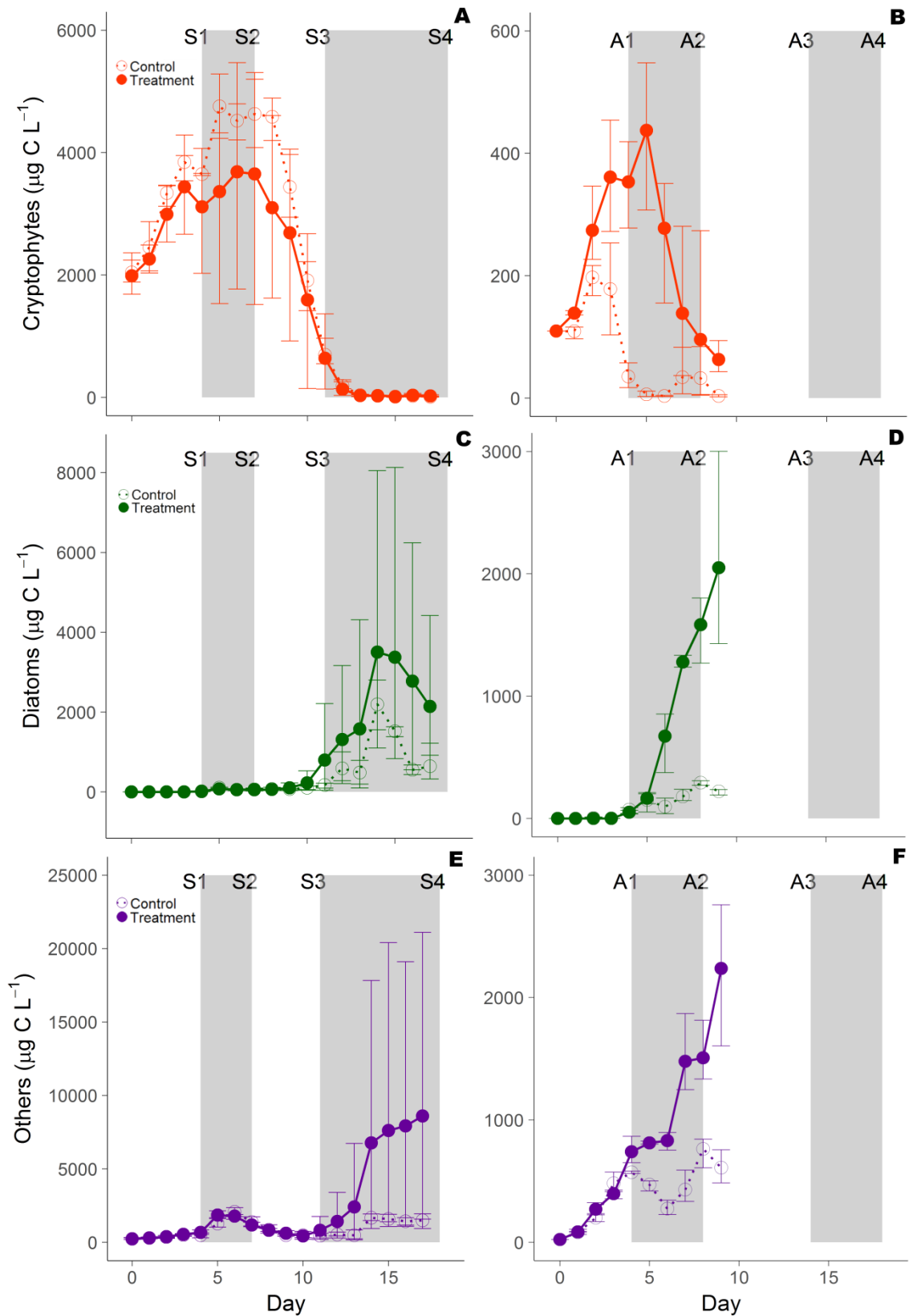


Figure 2. Phytoplankton biomass (chlorophyll *a*) and physiological state (C:Chla) temporal dynamics in spring (left column) and autumn (right column) experiments. Note the difference in scaling between spring and autumn experiments. Error bars show maximum and minimum of replicated units. The different phases observed in the experiments are indicated with shaded background.

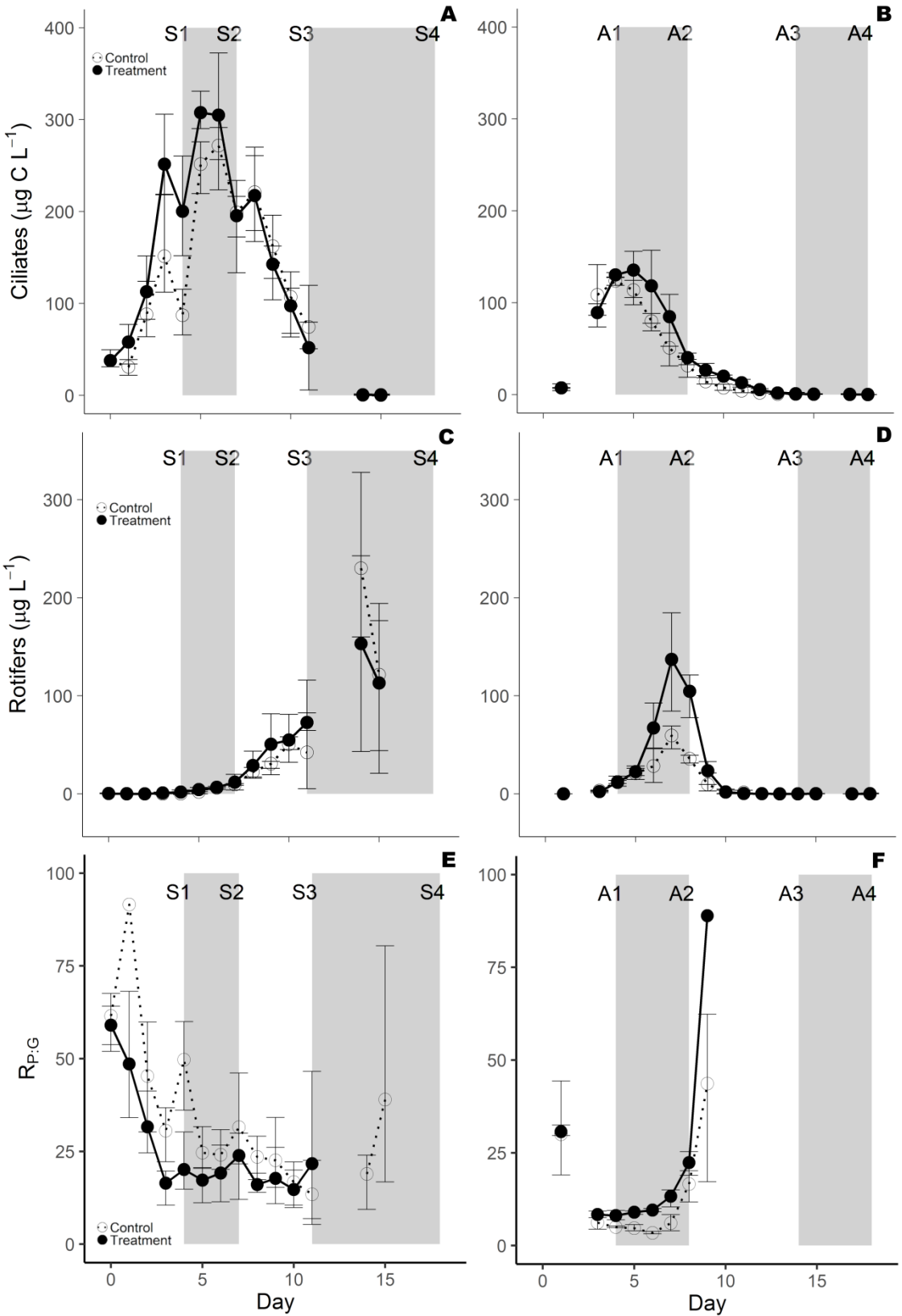


886 Figure 3. Temporal dynamics of the main phytoplankton groups in spring (left column)
 887 and autumn (right column) experiments. Note the difference in scaling between spring
 888 and autumn experiments. Error bars show maximum and minimum of replicated units.
 889 The different phases observed in the experiments are indicated with shaded background.



890

891 Figure 4. Ciliates and rotifer biomasses and the biomass ratio of phytoplankton to
 892 grazers ($R_{P:G}$) in spring (left column) and autumn (right column) experiments. Error
 893 bars show maximum and minimum of replicated units. The different phases observed in
 894 the experiments are indicated with shaded background.



895

896 Figure 5. Free-living bacteria abundances in spring (a) and autumn (b). Error bars show
 897 maximum and minimum of replicated units. The different phases of the experiments are
 898 indicated with shaded background.

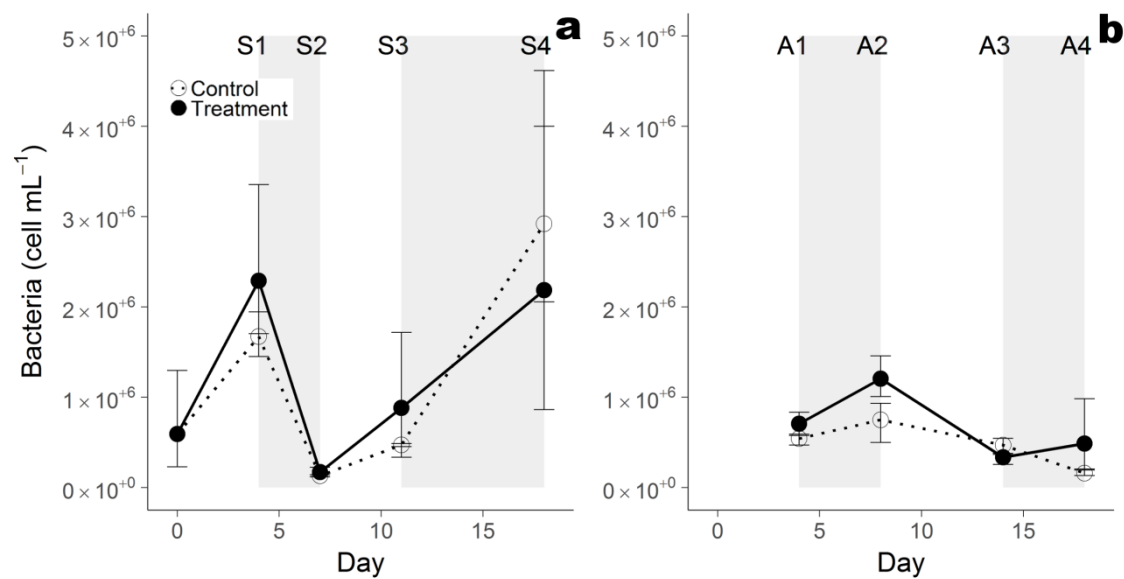
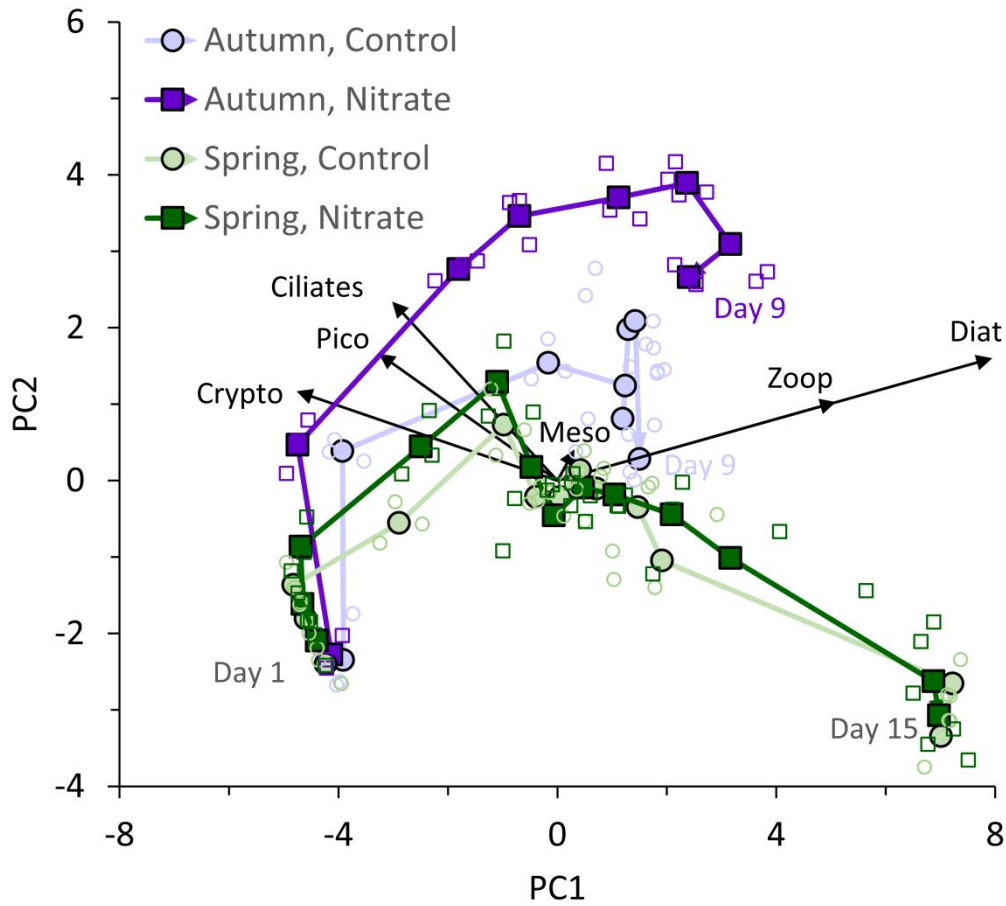
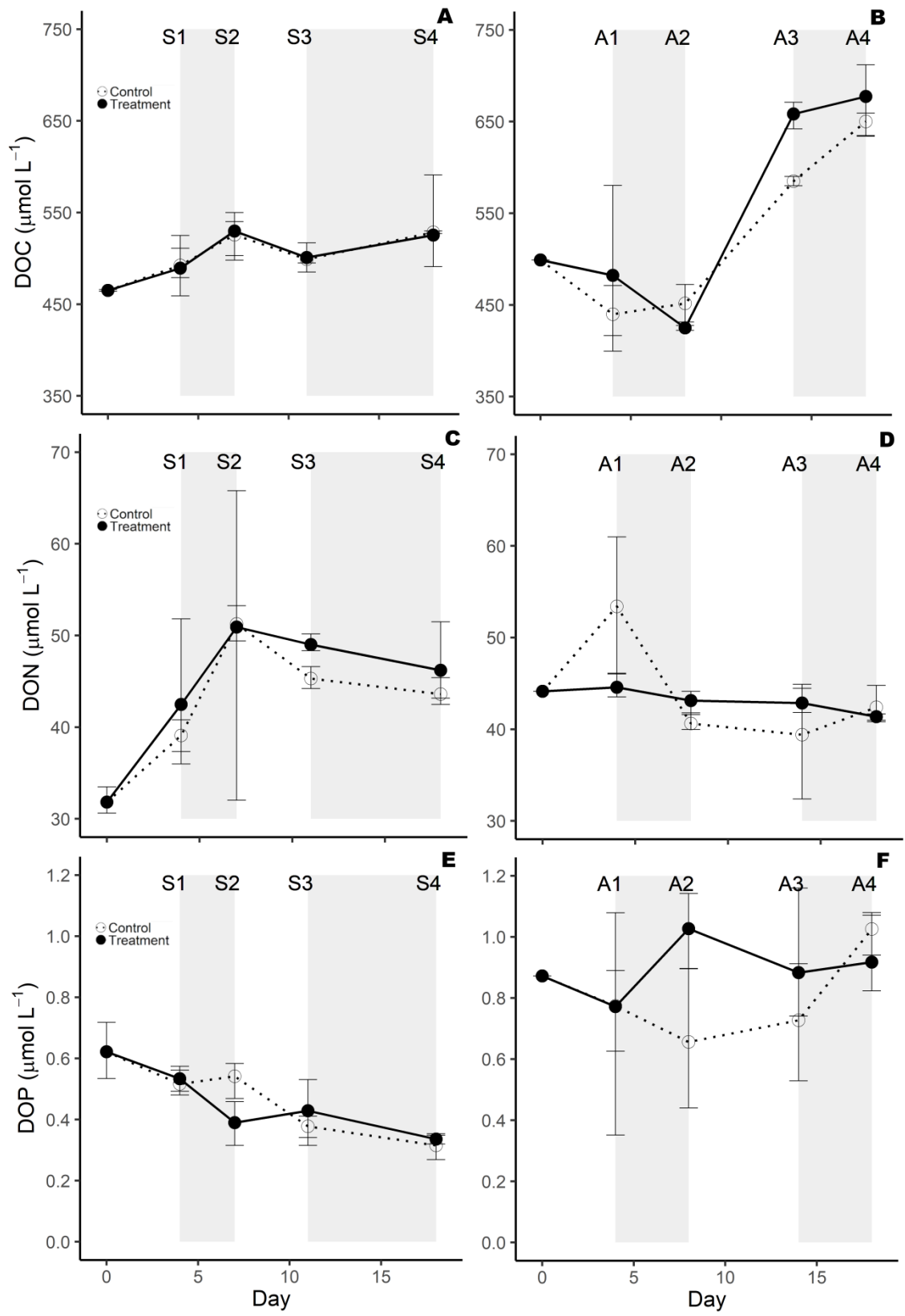


Figure 6. Trajectories of planktonic components over the course of the experiments obtained from Principal Components Analysis (PCA). Empty circles represent the individual observations and filled symbols show daily averages across the triplicate experimental units. Loadings of PC1 and PC2 are shown with arrows: Crypto = cryptophytes, Pico = pico-eukaryotes, Ciliates = ciliates, Meso = *Mesodinium rubrum*, Zoop = rotifers, and Diat = diatoms.

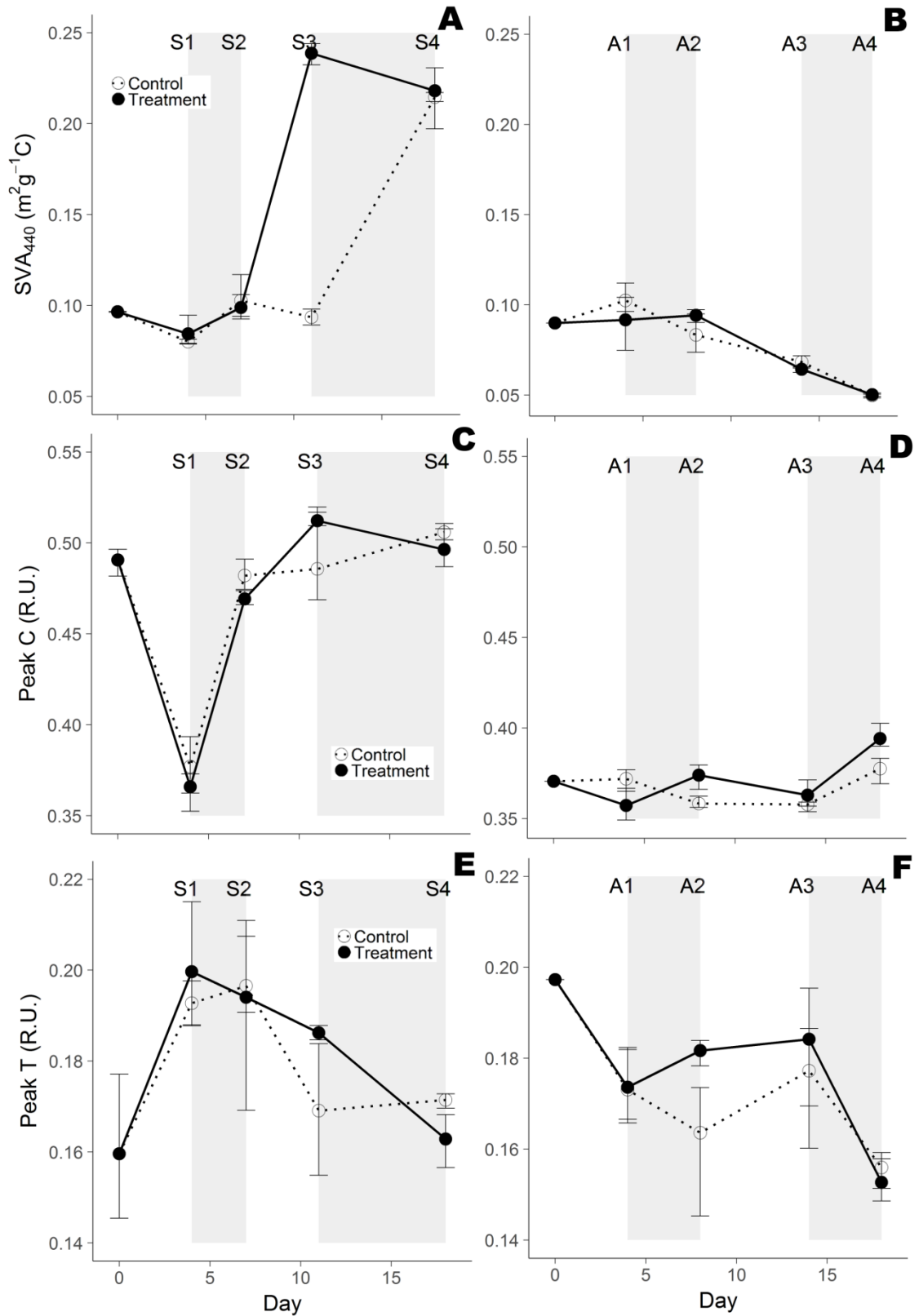


907 Figure 7. Dissolved organic carbon, nitrogen and phosphorus concentrations in spring
 908 (left column) and autumn (right column) experiments. Error bars show maximum and
 909 minimum of replicated units. The different phases observed in the experiments are
 910 indicated with shaded background.



911

912 Figure 8. CDOM (SVA₄₄₀) and FDOM (peak C and peak T) components in spring (left
 913 column) and autumn (right column) experiments. Error bars show maximum and
 914 minimum of replicated units. The different phases observed in the experiments are
 915 indicated by the shaded background colours.



916

917

Table SI: Significant rates of change ($P < 0.05$) derived from the repeated measures mixed model for the different phases of the two seasonal experiments, for the plankton community components and FDOM variables. Rates were estimated as the difference between start and end day divided by number of days. For phytoplankton, microzooplankton and bacteria response variables, rates are expressed as relative changes per day. Non-significant rates ($P > 0.05$) are not shown. Phases with a significant change in rates between control (C) and treatment (T) are shaded in grey.

Spring experiment	Phases							
	S1		S2		S3		S4	
	C	T	C	T	C	T	C	T
C _{cryptophytes} (% d ⁻¹)					-38%	-40%	-52%	-40%
C _{diatoms} (% d ⁻¹)	85%	108%	81%			48%	22%	39%
C _{others} (% d ⁻¹)		37%	53%		-43%	-32%		
C _{ciliates} (% d ⁻¹)	23%	51%	31%		-23%	-35%	-63%	-54%
C _{rotifers} (% d ⁻¹)			107%	69%		61%	58%	
A _{bacteria} (% d ⁻¹)	41%	51%	-57%	-58%	38%	43%	29%	
Peak-C (R.U. d ⁻¹)	-0.028	-0.031	0.035	0.034		0.011		
Peak-T (R.U. d ⁻¹)	0.008	0.010			-0.007			-0.003
Autumn experiment	A1		A2		A3		A4	
	C	T	C	T	C	T	C	T
C _{cryptophytes} (% d ⁻¹)	-26%			-48%	-76%			
C _{diatoms} (% d ⁻¹)	188%	167%	43%	136%				
C _{others} (% d ⁻¹)	43%	96%		-14%		-47%		
C _{ciliates} (% d ⁻¹)	152%	151%	-29%	-25%	-39%	-41%		
C _{rotifers} (% d ⁻¹)	136%	128%	29%	72%	-45%	-54%		
A _{bacteria} (% d ⁻¹)						-19%	-24%	
Peak-C (R.U. d ⁻¹)		-0.003	-0.003	0.004		-0.002	0.005	0.008
Peak-T (R.U. d ⁻¹)	-0.006	-0.006					-0.005	-0.008